

ATTACHMENT C

GE Nuclear Energy Report GE-NE-B13-02097-00, Section 5-Rev. 1

**The Evaluation of Observed Cracking at Nine Mile Point Unit 1
H9 Weld for Continued Operation**

(Non-Proprietary Version)



GE Nuclear Energy

**TECHNICAL SERVICES
GE Nuclear Energy
175 Curtner Avenue, San Jose, CA 95125**

***GE-NE-B13-02097-00, Section 5-Rev. 1
DRF #B13-02097-00, Section 5
Class I
July 2001***

THE EVALUATION OF OBSERVED CRACKING AT NINE MILE POINT UNIT 1 H9 WELD FOR CONTINUED OPERATION

July 2001

Prepared for

**Niagara Mohawk
Nine Mile Point 1**





GE Nuclear Energy

175 Curtner Avenue, San Jose, CA 95125

*GE-NE-B13-02097-00, Section 5-Rev. 1
DRF #B13-02097-00, Section 5
Class I
July 2001*

**THE EVALUATION OF OBSERVED CRACKING AT NINE
MILE POINT UNIT 1 H9 WELD FOR CONTINUED
OPERATION**

July 2001

Prepared by:

H. S. Mehta
R. M. Horn

Approved: _____

**R.M Horn, Manager
Structural Mechanics & Materials**

PROPRIETARY INFORMATION NOTICE

This is a non-proprietary version of the document GENE-B13-02097-00, Section 5-00, Rev.1, which has proprietary information deleted. The deleted information is identified by sidebars in the right margin next to the affected text, tables and figures. This paragraph has a sidebar as an example.

DISCLAIMER OF RESPONSIBILITY

Important Notice Regarding the Contents of this Report

Please Read Carefully

The only undertaking of General Electric Company respecting information in this document are contained in the contract between NMPC and General Electric Company, and nothing contained in this document shall be construed as changing the contract. The use of this information by anyone other than NMPC or for any purpose other than that for which it is intended is not authorized; and with respect to any unauthorized use, General Electric Company makes no representation or warranty, and assumes no liability as to the completeness, accuracy, or usefulness of the information contained in this document.

Table of Contents

<u>Subject</u>	<u>Page No.</u>
1. EXECUTIVE SUMMARY	1
2. BACKGROUND AND SUMMARY OF H9 CRACK INDICATIONS	2
2.1. BACKGROUND.....	2
2.2. REFERENCES.....	3
3. SHROUD SUPPORT STRUCTURAL MARGIN ASSESSMENT	4
3.1. STRUCTURAL EVALUATION METHODOLOGY	4
3.2. CONCLUSION FROM DLL STRUCTURAL MARGIN EVALUATION.....	5
3.3. REFERENCES.....	5
4. H9 STRUCTURAL INTERGRITY METHODOLOGY APPLICABILITY REVIEW	11
5. EVALUATION OF NMP-1 FINDINGS ON CURRENT UNDERSTANDING OF SHROUD SUPPORT CRACKING	13
5.1. IMPACT EVALUATION.....	13
5.2. REFERENCES.....	15
6. NMCA (NOBLECHEM™) EFFECTIVENESS FOR SHROUD SUPPORT CRACKING AT NMP-1.....	20
7. IMPACT OF ALLOY 182 CRACKING ON THE REACTOR PRESSURE VESSEL	27
7.1. BACKGROUND.....	27
7.2. STRESS DISTRIBUTIONS	28
7.3. K CALCULATIONS	29
7.4. CRACK GROWTH CALCULATIONS	30
7.5. IWB-3600 EVALUATION.....	31
7.6. REFERENCES.....	31
8. REINSPECTION RECOMMENDATIONS	42
9. CONCLUSIONS	42

List of Tables

Table 3-1	Circumferential Indications	6
Table 3-2	DLL Un-cracked Section Input	7
Table 3-3	DLL Run for H9 Weld	8
Table 7-1	Stresses Due to Internal Pressure and Temperature in the RPV at H9 Weld.....	32
Table 7-2	Coefficients for K calculation.....	32

List of Figures

Prepared by:..... i

Figure 4-1 180° Model of RPV and Shroud Support With Moment Loading and Boundary Conditions Applied..... 12

Figure 5-1: Schematic of the circumferential orientation and length of the H9 indications as determined by UT in the March 2001 inspection. 16

Figure 5-2: Schematic of the weld buildup for the H9 weld in a BWR/2 plant. The dendritic orientation is indicated by the direction of the cross-hatched markings... 17

Figure 5-3: Schematic of the indications in the Tsuruga H9 weld region showing a series of circumferential indications that would overlap, having a UT length of 4-5 degrees 18

Figure 5-4: Replica metallography from circumferential crack and axial crack in the Tsuruga H9 weld region. The circumferential and axial cracking can be clearly linked due to the weld metal microstructure. 19

Figure 6-1: K-dependent Disposition Curve for Alloy 182 in HWC at or below Action Level 1 23

Figure 6-2: The effect of corrosion potential on the crack growth rate of Alloy 182 weld metal in near-theoretical purity water. The shift to H₂-deaerated conditions produces an immediate and dramatic decrease in growth rate. 24

Figure 6-3. Crack length vs. time for Alloy 182 weld metal tested in 288 °C water containing 95 ppb H₂ showing the very well behaved nature of many of the crack growth observations at low corrosion potential / low crack growth rates. The measured rate is less than 5×10^{-9} mm/s (7×10^{-7} in/hr) at the low corrosion potential typical of HWC with NobelChem™. 25

Figure 6-4: Comparison of Crack Growth Rates in Alloy 182 made using the PLEDGE Model. The benefit of HWC (-230mV, she) is clearly shown by the lower line. 26

Figure 7-1 Axisymmetric Finite Element Model of RPV Including The Conical Shroud Support 33

Figure 7-2 Axial (Y) Stress Distribution Due to Pressure and Temperature at Normal Operation..... 34

Figure 7-3 Circumferential (Z) Stress Distribution Due to Pressure and Temperature at Normal Operation 35

Figure 7-4: Assumed Clad Residual Stress Distribution 36

Figure 7-5 Assumed Weld Residual Stress Distribution..... 37

Figure 7-6 Edge Cracked Plate Model for K Calculation Due to Clad Stress 38

Figure 7-7 K Due to Clad Stress and Polynomial Fit..... 39

Figure 7-8 Calculated Values of Total K and the Polynomial Fit..... 40

Figure 7-9: Crack Growth Prediction as a Function of Operating Hours..... 41

1. EXECUTIVE SUMMARY

Shroud support weld examinations were performed during the RF016 outage at Nine Mile Point Unit 1 (NMP-1). These ultrasonic (UT) examinations were performed from the upper conical support plate surface for all accessible areas of welds H8 and H9. The evaluation of crack indications detected at the H9 weld is the subject of this report.

Section 2 of this report provides background on the H9 weld cracking observed in a similar BWR reactor vessel and a summary of the inspection findings at NMP-1. Section 3 describes evaluation results on the structural margin available at the H9 weld to support the loading from the shroud. The methodology followed is that provided in BWRVIP-38. Projected crack growth based on 10 years (approximately 80,000 hours) of operation was included in the evaluation. The results showed that the safety factor is 12.53 compared to the minimum required safety factor of 1.39. The BWRVIP-38 methodology was intended for circumferential cracking only. The observed cracking at the H9 weld may also include some axial cracking. Section 4 includes the results of finite element analyses on NMP-1 RPV geometry to demonstrate that the presence of axial cracking has insignificant impact on the BWRVIP-38 circumferential flaw tolerance methodology.

Section 5 addresses the impact of the NMP-1 inspection findings on the GE SIL 624 metallurgical assessment that describes previous conditions at Tsuruga involving primarily axial cracking. Section 6 presents current data that confirms the effectiveness of NobleChemTM (NMCA) in mitigating SCC growth in the Alloy 182 weld material used in the construction of the H9 weld.

Section 7 presents the results of an assessment of the potential for cracking progressing into the low alloy steel. This NMP-1 specific assessment was performed using the fracture mechanics methodology and crack growth relationships consistent with those outlined in BWRVIP-60. The evaluation showed that crack depth in the reactor wall is predicted to be less than the allowable value even after an operating period in excess of 100,000 hours. This result, in conjunction with the evaluation result of Section 3, justifies continued operation of NMP-1 with the observed H9 weld cracks for at least 5 additional operating cycles, equivalent to 10 years operation. Section 8 briefly provides inspection recommendations consistent with BWRVIP-74 and section 9 provides conclusions.

2. BACKGROUND AND SUMMARY OF H9 CRACK INDICATIONS

2.1. BACKGROUND

Stress corrosion cracks were discovered in Alloy 182 welds in late 1999 in the shroud support structure of Tsuruga-1, a GE BWR-2 located in Japan. This weld material was used in the construction of the conical support structure as well as to attach the support structure to the reactor pressure vessel (RPV). These cracks were detected visually and confirmed with penetrant inspection as well as by metallography during core shroud replacement activities. The number of crack indications was more extensive than had been seen previously in BWRs and the cracks were located on the underside of the core support structure. Finally, many of the cracks that were found occurred at the H9 weld location, the attachment weld of the shroud support to the RPV.

Following this finding, GE recommended that BWR owners review their inservice inspection programs and consider performing an examination of this RPV to shroud support plate H9 weld [Reference 2-1]. In addition to these inspections, it was also acknowledged in Reference 2-1 that there are significant benefits from operating with hydrogen water chemistry (HWC) in conjunction with NobleChemTM.

In line with these recommendations, NMP-1 performed a ultrasonic (UT) examination of the H9 weld. These examinations were conducted to assess the presence of circumferential crack indications, the flaw orientation that is of most significance to the function of the shroud support structure. The inspection was limited to circumferential direction because the UT deployed from inside the vessel was not capable of axial direction. These inspections were performed by GE Inspection Services. A total of 287 degrees of the circumference was examined. A total of 34 indications were found with a total combined length of 51.5 degrees. Of these 34 indications, only 4 had similar amplitudes to the implanted flaws in the UT demonstration mockup. All other indications had lower amplitude, indicative of the flaw indications being shallower or being oriented differently from the circumferential mockup flaws. Thus, it is likely that only four of the 34 indications are significant circumferential flaws and the remaining 30 are either very shallow or not circumferentially oriented. Table 3-1, in Section 3, lists the UT indication location and lengths (taken from Reference 2-3, which gives the details of the inspections performed).

The purpose of this report is to detail the analyses that support continued operation of NMP-1 for multiple cycles with these indications. The report also provides discussion of the metallurgical implications of the UT indications as well as discussion of

the benefit in mitigating cracking in Alloy 182 with hydrogen water chemistry with noble metal chemical addition (HWC/NMCA)

2.2. REFERENCES

- [2-1] "Stress Corrosion Cracking in Alloy 182 Welds in Shroud Support Structure," GE Service Information Letter No. 624, March 24, 2000.
- [2-2] BWR Shroud Support Inspection and Flaw Evaluation Guidelines (BWRVIP-38), EPRI Report No. TR-108823, September 1997.
- [2-3] "Nine Mile Point Unit 1, Shroud Support Ultrasonic Examinations," Prepared for Niagara Mohawk, GE Report No. 01-KCNES-JKWWZ, March 2001.

3. SHROUD SUPPORT STRUCTURAL MARGIN ASSESSMENT

This section presents the structural integrity evaluation of the conical shroud support in the presence of the observed cracking at the H9 weld. The bulk of the observed cracking at the H9 weld is assumed to be circumferentially oriented with some potential axial indications. BWRVIP-38 provides the methodology for the structural integrity evaluation of the H9 weld in the presence of circumferential cracking. A justification for the use of this methodology in cases where axial cracking is also present is provided in Section 4.

3.1. STRUCTURAL EVALUATION METHODOLOGY

The DLL (Distributed Ligament Length) computer program [Reference 3-1] is based on the limit load approach. The calculated values of primary membrane (P_m) and primary bending stresses (P_b) were those reported in Reference 3-2 as a part of input provided for BWRVIP-38 [Reference 2-2]. The following table lists the P_m and P_b stresses for upset and faulted conditions:

Operating Condition	Primary Stresses (psi)	
	P_m	P_b
Upset	638	1149
Faulted	1875	1149

It was determined that the faulted condition stresses are governing in terms of structural margin. Thus, the values used in the DLL run are the following:

$$P_m = 1875 \text{ psi}$$

$$P_b = 1149 \text{ psi}$$

The beginning and end azimuth values of the indications are shown in Table 3-1 along with the beginning and end azimuth values of the un-inspected areas. The evaluation factor and RMS values (in inch units) are the following [Reference 3-3]:

	<u>NDE</u>	<u>Tooling</u>
RMS	0.842	0.012
Evaluation	0.421	0.006

Based on the above information, each end of an indication was extended by $(0.421+0.006)$ or 0.427 inch. Additionally, a crack growth rate of 5×10^{-5} inch/hour was conservatively used to grow the indications for an operating period of 10 years ($\approx 80,000$ hours). To account for the possibility that indications may be present at both ends of the

un-inspected regions, these regions were also allowed to grow at the same rate as the indications in the inspected regions.

Following this step, a proximity criterion was applied to combine neighboring indications. By this criterion, two indications that were less than '2t' apart (thickness 't' being equal to the nominal thickness of the cone, 1.5 inches) were combined into one indication with the in-between ligament assumed as cracked. Table 3-2 shows the final beginning and end azimuth values of the remaining un-cracked metal after accounting for the measurement uncertainty, growth and the application of the proximity criterion to the detected indications at weld H9. These values are used in the DLL evaluation. Table 3-3 shows the output from the DLL program indicating the structural margin at various azimuth values. It is seen that a minimum safety factor of 12.53 is indicated. The minimum required safety factor is 1.39 for the emergency/faulted conditions. Thus, it is shown that sufficient structural margin at H9 weld exists following 10 years or 80,000 hours of plant operation.

3.2. CONCLUSION FROM DLL STRUCTURAL MARGIN EVALUATION

Based on the preceding evaluation results it is concluded operation for at least 5-2 year fuel cycles or approximately 10 years is justified.

3.3. REFERENCES

- [3-1] BWRVIP Core Shroud Distributed Ligament Length (DLL) Computer Program (Version 2.1) (BWRVIP-20), EPRI Report No. AP-107283, December 1996.
- [3-2] "Shroud Support Redundancy Analysis and Third Party Review," GE Design Record File No. B13-01805-71.
- [3-3] Tables 1 and 2 from GE Demonstration of UT techniques for BWRVIP: Phased Array Inspection of BWR/2 Welds H8 and H9.

Table 3-1 Circumferential Indications

Indication No.	Start, Degrees	End, Degrees
1	-2.17	-1.61
2	21.91	22.61
3	55.65	56.77
4	58.45	60.41
5	63.07	64.47
6	64.89	66.01
7	72.45	74.27
8	75.39	76.66
9	117.99	118.55
10	135.35	136.19
11	147.53	147.95
12	148.65	150.47
13	152.71	153.69
14	172.99	173.69
15	173.97	177.05
16	177.61	178.31
17	192.03	196.09
18	196.23	197.07
19	197.63	201.97
20	203.23	207.29
21	208.55	208.97
22	211.35	212.75
23	222.13	224.09
24	234.59	235.85
25	243.83	245.79
26	248.73	250.97
27	256.01	256.57
28	256.71	257.13
29	257.83	258.81
30	318.01	318.85
31	324.59	327.95
32	328.23	328.65
33	331.87	332.71
34	336.49	339.01

Un-inspected Regions

Start Degrees	End Degrees
77.49	96.99
154.53	172.99
260.49	276.99
339.01	357.69

Table 3-2 DLL Un-cracked Section Input

Region	Theta1 (Degrees)	Theta2 (Degrees)
1	0.8	19.5
2	25	53.3
3	99.4	115.6
4	120.9	133
5	138.6	145.1
6	180.7	189.6
7	215.1	219.7
8	226.5	232.2
9	238.2	241.4
10	279.4	315.6

Table 3-3 DLL Run for H9 Weld

DLL: DISTRIBUTED LIGAMENT LENGTH EVALUATION, REV. 2.1 (09/19/96)
 DATE OF THIS ANALYSIS: 04/11/2001

SUMMARY OF INPUTS:

=====
 Title: NMP-1 H9 LL 10 years
 Angle increment = 1.0 deg. (COARSE)
 Membrane Stress, Pm = 1875. psi
 Bending Stress, Pb = 1149. psi
 Safety Factor, SF = 1.39
 Mean Radius, Rm = 105.94 inches
 Wall Thickness, t = 1.500 inches
 Stress Intensity, Sm = 23300. psi
 Fluence = 0.0E+00 n/cm^2
 (Thus, LEFM evaluation not applicable)

REGION	THETA1 [deg.]	THETA2 [deg.]	THICKNESS [inches]
1	0.8	19.5	1.500
2	25.0	53.3	1.500
3	99.4	115.6	1.500
4	120.9	133.0	1.500
5	138.6	145.1	1.500
6	180.7	189.6	1.500
7	215.1	219.7	1.500
8	226.5	232.2	1.500
9	238.2	241.4	1.500
10	279.4	315.6	1.500

LIMIT LOAD RESULTS:

NOTE: THE FOLLOWING LIMIT LOAD RESULTS ASSUME THAT THE FLAWS TAKE COMPRESSION.

ALPHA [deg]	MOMENT Pb' [in-lbs]	SAFETY [psi]	FACTOR	RESULT
.0	2.163E+09	40898.	14.14	---->ACCEPTABLE
5.0	2.229E+09	42136.	14.55	---->ACCEPTABLE
10.0	2.274E+09	42995.	14.84	---->ACCEPTABLE
15.0	2.333E+09	44119.	15.21	---->ACCEPTABLE
20.0	2.388E+09	45152.	15.55	---->ACCEPTABLE
25.0	2.437E+09	46087.	15.86	---->ACCEPTABLE
30.0	2.481E+09	46917.	16.13	---->ACCEPTABLE
35.0	2.519E+09	47635.	16.37	---->ACCEPTABLE
40.0	2.551E+09	48237.	16.57	---->ACCEPTABLE
45.0	2.591E+09	48989.	16.82	---->ACCEPTABLE
50.0	2.599E+09	49138.	16.87	---->ACCEPTABLE
55.0	2.619E+09	49516.	16.99	---->ACCEPTABLE

60.0	2.625E+09	49628.	17.03	---->ACCEPTABLE
65.0	2.657E+09	50230.	17.23	---->ACCEPTABLE
70.0	2.685E+09	50761.	17.41	---->ACCEPTABLE
75.0	2.670E+09	50479.	17.31	---->ACCEPTABLE
80.0	2.679E+09	50661.	17.37	---->ACCEPTABLE
85.0	2.716E+09	51353.	17.60	---->ACCEPTABLE
90.0	2.714E+09	51321.	17.59	---->ACCEPTABLE
95.0	2.743E+09	51864.	17.77	---->ACCEPTABLE
100.0	2.741E+09	51834.	17.76	---->ACCEPTABLE
105.0	2.741E+09	51819.	17.76	---->ACCEPTABLE
110.0	2.775E+09	52470.	17.97	---->ACCEPTABLE
115.0	2.779E+09	52536.	17.99	---->ACCEPTABLE
120.0	2.775E+09	52475.	17.97	---->ACCEPTABLE
125.0	2.765E+09	52286.	17.91	---->ACCEPTABLE
130.0	2.749E+09	51972.	17.81	---->ACCEPTABLE
135.0	2.726E+09	51535.	17.66	---->ACCEPTABLE
140.0	2.673E+09	50531.	17.33	---->ACCEPTABLE
145.0	2.671E+09	50501.	17.32	---->ACCEPTABLE
150.0	2.651E+09	50128.	17.20	---->ACCEPTABLE
155.0	2.609E+09	49330.	16.93	---->ACCEPTABLE
160.0	2.618E+09	49503.	16.99	---->ACCEPTABLE
165.0	2.585E+09	48867.	16.78	---->ACCEPTABLE
170.0	2.548E+09	48168.	16.55	---->ACCEPTABLE
175.0	2.542E+09	48055.	16.51	---->ACCEPTABLE
180.0	2.491E+09	47092.	16.19	---->ACCEPTABLE
185.0	2.486E+09	47014.	16.17	---->ACCEPTABLE
190.0	2.479E+09	46871.	16.12	---->ACCEPTABLE
195.0	2.465E+09	46614.	16.03	---->ACCEPTABLE
200.0	2.434E+09	46026.	15.84	---->ACCEPTABLE
205.0	2.398E+09	45343.	15.61	---->ACCEPTABLE
210.0	2.357E+09	44560.	15.36	---->ACCEPTABLE
215.0	2.310E+09	43684.	15.07	---->ACCEPTABLE
220.0	2.259E+09	42721.	14.75	---->ACCEPTABLE
225.0	2.176E+09	41140.	14.22	---->ACCEPTABLE
230.0	2.149E+09	40631.	14.06	---->ACCEPTABLE
235.0	2.095E+09	39604.	13.72	---->ACCEPTABLE
240.0	2.048E+09	38724.	13.43	---->ACCEPTABLE
245.0	2.011E+09	38015.	13.19	---->ACCEPTABLE
250.0	1.965E+09	37147.	12.90	---->ACCEPTABLE
255.0	1.925E+09	36390.	12.65	---->ACCEPTABLE
260.0	1.910E+09	36108.	12.56	---->ACCEPTABLE
265.0	1.905E+09	36026.	12.53	---->ACCEPTABLE
270.0	1.912E+09	36144.	12.57	---->ACCEPTABLE
275.0	1.953E+09	36933.	12.83	---->ACCEPTABLE
280.0	1.952E+09	36908.	12.82	---->ACCEPTABLE
285.0	1.966E+09	37174.	12.91	---->ACCEPTABLE
290.0	1.977E+09	37387.	12.98	---->ACCEPTABLE
295.0	1.985E+09	37534.	13.03	---->ACCEPTABLE
300.0	1.989E+09	37617.	13.06	---->ACCEPTABLE
305.0	1.990E+09	37632.	13.06	---->ACCEPTABLE
310.0	1.988E+09	37582.	13.05	---->ACCEPTABLE
315.0	1.968E+09	37206.	12.92	---->ACCEPTABLE
320.0	1.979E+09	37426.	13.00	---->ACCEPTABLE
325.0	1.948E+09	36834.	12.80	---->ACCEPTABLE

330.0	1.954E+09	36938.	12.83	---->ACCEPTABLE
335.0	1.984E+09	37507.	13.02	---->ACCEPTABLE
340.0	2.018E+09	38164.	13.24	---->ACCEPTABLE
345.0	2.044E+09	38646.	13.40	---->ACCEPTABLE
350.0	2.060E+09	38951.	13.50	---->ACCEPTABLE
355.0	2.100E+09	39711.	13.75	---->ACCEPTABLE

ACCEPTABLE! MINIMUM SAFETY FACTOR = 12.53 AT 265.0 DEGREES.

4. H9 STRUCTURAL INTEGRITY METHODOLOGY APPLICABILITY REVIEW

The circumferential flaw tolerance analyses for the H9 weld reported in BWRVIP-38 do not consider the impact of axial cracking that may be present at this weld. Although no axial cracking at the H9 weld has been definitely identified at NMP-1 by the UT inspection conducted during the RFO-16 outage, the presence of some axial cracking at this weld cannot be ruled out. Therefore, an evaluation was conducted to determine the effect of axial cracking on the BWRVIP-38 circumferential flaw evaluation methodology.

Two 180° models of the NMP-1 conical shroud support structure including a section of the RPV wall were prepared. One of the models considered only the circumferential cracking represented. The circumferential cracking modeled included crack growth after 10-years of operation. The second model considered axial through-wall cracks at the H9 weld in addition to the circumferential cracking considered in the first model (see Figure 4-1). The axial cracks were modeled every 1° of the azimuth and had a length equal to two times the nominal thickness of the shroud support cone. A varying vertical force simulating a moment loading was applied at the top of the shroud cylinder in each model. Based on the peak displacement obtained at the same location, a compliance value was calculated for each model.

Based on a comparison between the results of the two models, it was determined that the compliance of the model with postulated axial cracks was less than 4% higher than the model without the axial cracks. This change in compliance was not considered significant and thus it was concluded that the presence of axial cracking, if any, would not affect the circumferential flaw tolerance evaluation at the H9 weld.

Thus the structural margin analysis results described in Section 3 remain valid even in the presence of axial cracking at the H9 weld.

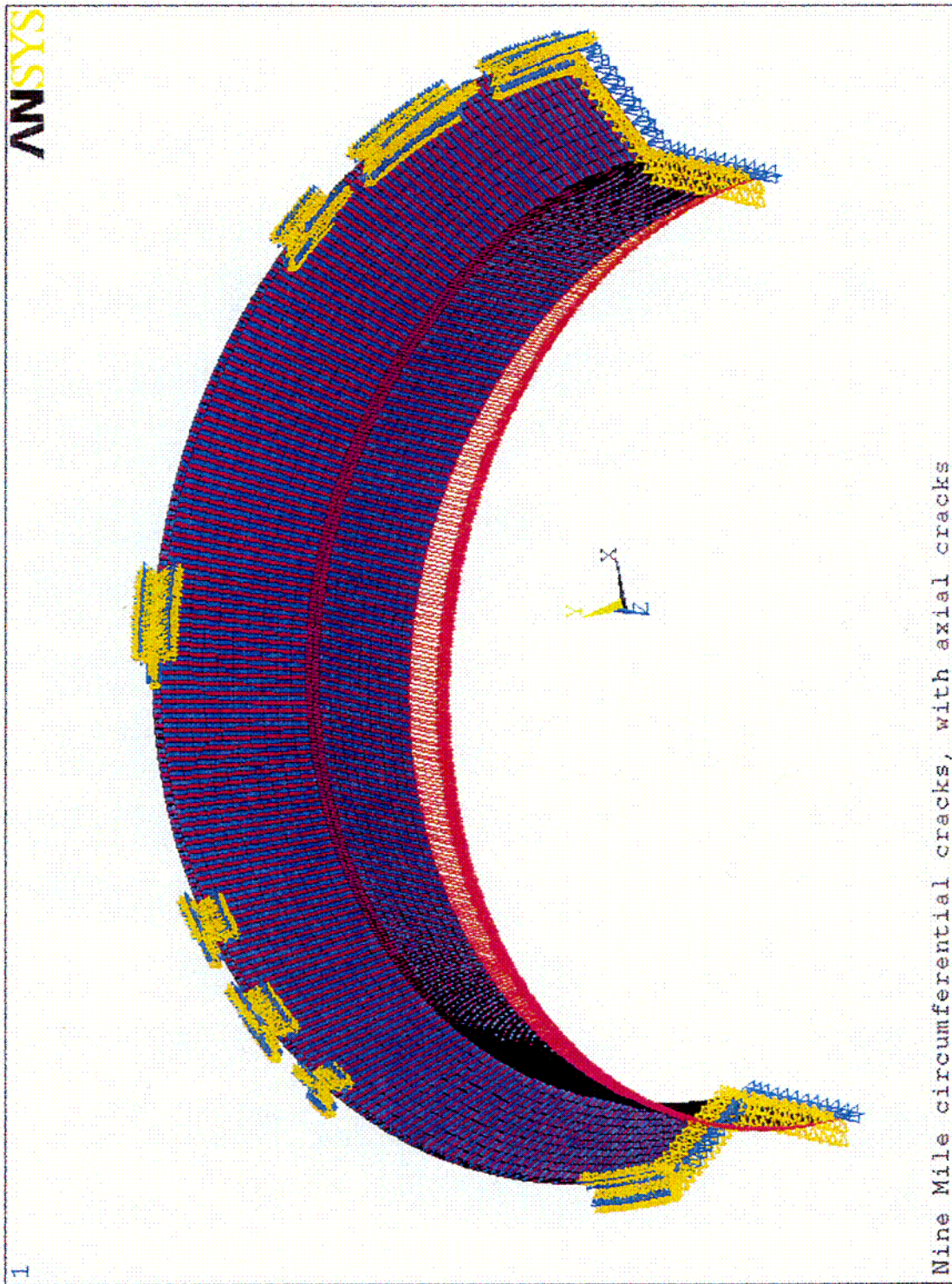


Figure 4-1 180° Model of RPV and Shroud Support With Moment Loading and Boundary Conditions Applied

5. EVALUATION OF NMP-1 FINDINGS ON CURRENT UNDERSTANDING OF SHROUD SUPPORT CRACKING

5.1. IMPACT EVALUATION

Based on the inspection findings at NMP-1, it is appropriate to review these findings in terms of the general cracking characteristics. This evaluation is best made on an assessment of the size and orientation of the crack indications as well as from the general characteristics of the microstructure and the expected orientation dependency of stress corrosion cracking (SCC) in the weld metal. The UT findings for the NMP-1 H9 weld are displayed in Figure 5-1 (data from Reference 2-3). This plot shows the circumferential crack indications that were found. Based on the inspection report, it can be seen that the majority of these 34 indications are 1.5 degrees or less in length and in three of four of the quadrants, the detected cracking is limited and fairly evenly spaced. Only in the 180 to 270 degree sector are there longer and more densely spaced UT indications. It is stated in the inspection report that all of the indications are located in the weld and initiate from the lower inside (i.d.) surface. Of these 34 indications, only 4 had amplitudes similar to those in the qualification mockup. The other indications had lower amplitude that may suggest that the flaws are either shallower or oriented differently than flaws within the BWRVIP mockup. While the UT examination was not able to better characterize the flaw orientation, it is possible that these 30 flaws could be axial or have axial components.

The existence of flaws with both circumferential and non-circumferential (e.g., axial) orientations is very consistent with the microstructure of Alloy 182 weld metal and the expected cracking patterns in this material. All of the columnar dendritic boundaries are potentially susceptible to SCC as shown schematically in Figure 5-2. Therefore, the orientation of the cracking will depend on the stress state. It is clear that both axial and circumferential cracking can occur since the residual stresses have been shown to be tensile in previous studies. The experiences of Alloy 182 cracking in nozzle butters have also established that while axial cracking may be more common, circumferential cracking can occur as discussed in BWRVIP-59 [Reference 5-1].

In that there is little metallurgical difference between the axial and circumferential orientation at the surface, it would also be expected that many cracks could also exhibit both characteristics or even skewed orientations. Figures 5-3 and 5-4 show examples from the Tsuruga-1 cracking [Reference 5-2]. Figure 5-3 displays the dye penetrant results and there are both axial and circumferential segments in the small part of the circumference shown. Likewise, Figure 5-4 presents photomicrographs from a boat sample that contained both orientations of cracking. For axial segments, the maximum length is limited by the thickness of the weld. For circumferential oriented cracking, it

would be expected that although the flaw could have substantial length, there would be low probability that the cracking would remain oriented in the circumferential orientation. This is in contrast to cracking in welded stainless steel where the cracking has been observed to be parallel to the weld fusion line in the narrow region of heat-affected zone.

The cracking found at Tsuruga-1 can also be compared with the NMP-1 indications. Since the examination at NMP-1 was directed at circumferential cracking only because of UT limitations, the comparison between the level and extent of circumferential cracking can also be separately evaluated out of the 228 crack indications found at Tsuruga on the H9 weld. The rollout of the PT indications shows that there were at least 21 circumferential cracks. Several of these indications were combined with axial segments or skewed crack segments. The largest number of cracks including circumferential segments was found in the 60° to 100° segment. This region is shown in Figure 5-3. It can be seen that the three cracks at ~80° overlapped and could be viewed as a continuous indication by UT from the top side of the shroud support cone. The length of these overlapping indications is ~4°, similar to the length found at NMP-1.

The available information [References 5-2 and 5-3] on analytically calculated weld residual stresses at the H9 weld following various stages of fabrication and pressure testing, was reviewed to determine if it can provide some insight into: (1) why the observed cracking at Tsuruga-1 was predominantly axial in nature while the UT revealed circumferential cracking at NMP-1 and (2) whether the weld residual stress distribution assumed in the BWRVIP-60 [Reference 5-4] and also used in this evaluation, is reasonable and perhaps conservative. The review of the Tsuruga-1 analysis showed that the magnitude of the axial stresses, while smaller than the circumferential stresses, is still large enough such that circumferential cracking would be found [Reference 5-3]. Therefore, it was concluded that cracks of both orientations (i.e., axial or circumferential) should be found at the H9 weld. The current interpretation of the indications, ~10% of the cracking definitely circumferential in orientation, is consistent with these analytical results. The review also showed that the weld residual stress distribution in BWRVIP-60 5-4 is conservative relative to the analytical results of Reference 5-3.

In summary, the findings associated with the NMP-1 H9 weld are consistent with our understanding of the microstructure of the susceptible Alloy 182 weld metal. The findings are also consistent with data gained on cracking orientation from Tsuruga-1, particularly the amount and relative extent of circumferentially oriented cracks. Therefore, the NMP-1 findings only add to, not change, the perspective of the information provided in GE SIL 624 [Reference 5-5].

5.2. REFERENCES

- [5-1] "BWR Vessel and Internals Project, Evaluation of Crack Growth in BWR Nickel Base Austenitic Alloys in RPV Internals (BWRVIP-59)," EPRI Report TR-108710, December 1998.
- [5-2] JAPC Web Page.
- [5-3] JAPC Proprietary data
- [5-4] "BWR Vessel and Internals Project, Evaluation of Stress Corrosion Crack Growth in Low Alloy Steel Vessel Materials in the BWR Environment (BWRVIP-60)," EPRI Report TR-108709, March 1999.
- [5-5] GE SIL 624, "Stress Corrosion Cracking in Alloy 182 Welds in Shroud Support Structure," March 24, 2000.

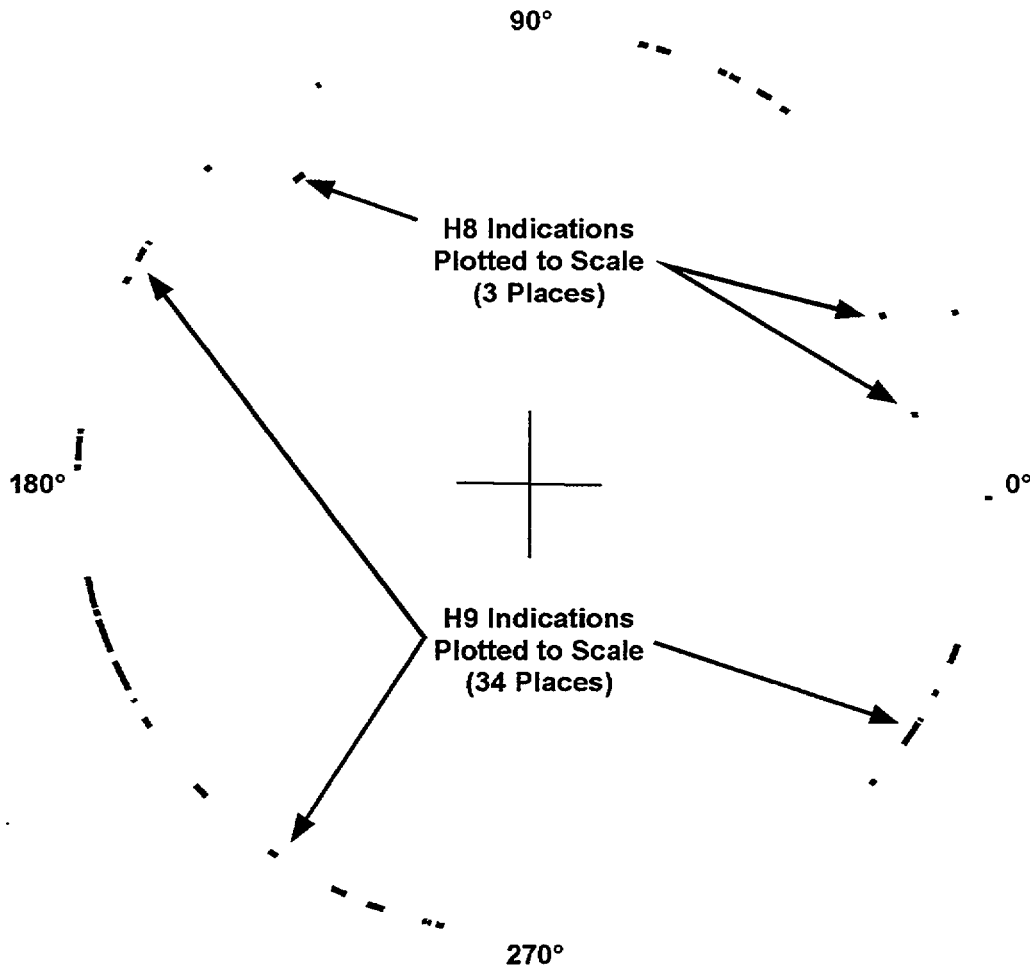


Figure 5-1: Schematic of the circumferential orientation and length of the H9 indications as determined by UT in the March 2001 inspection.

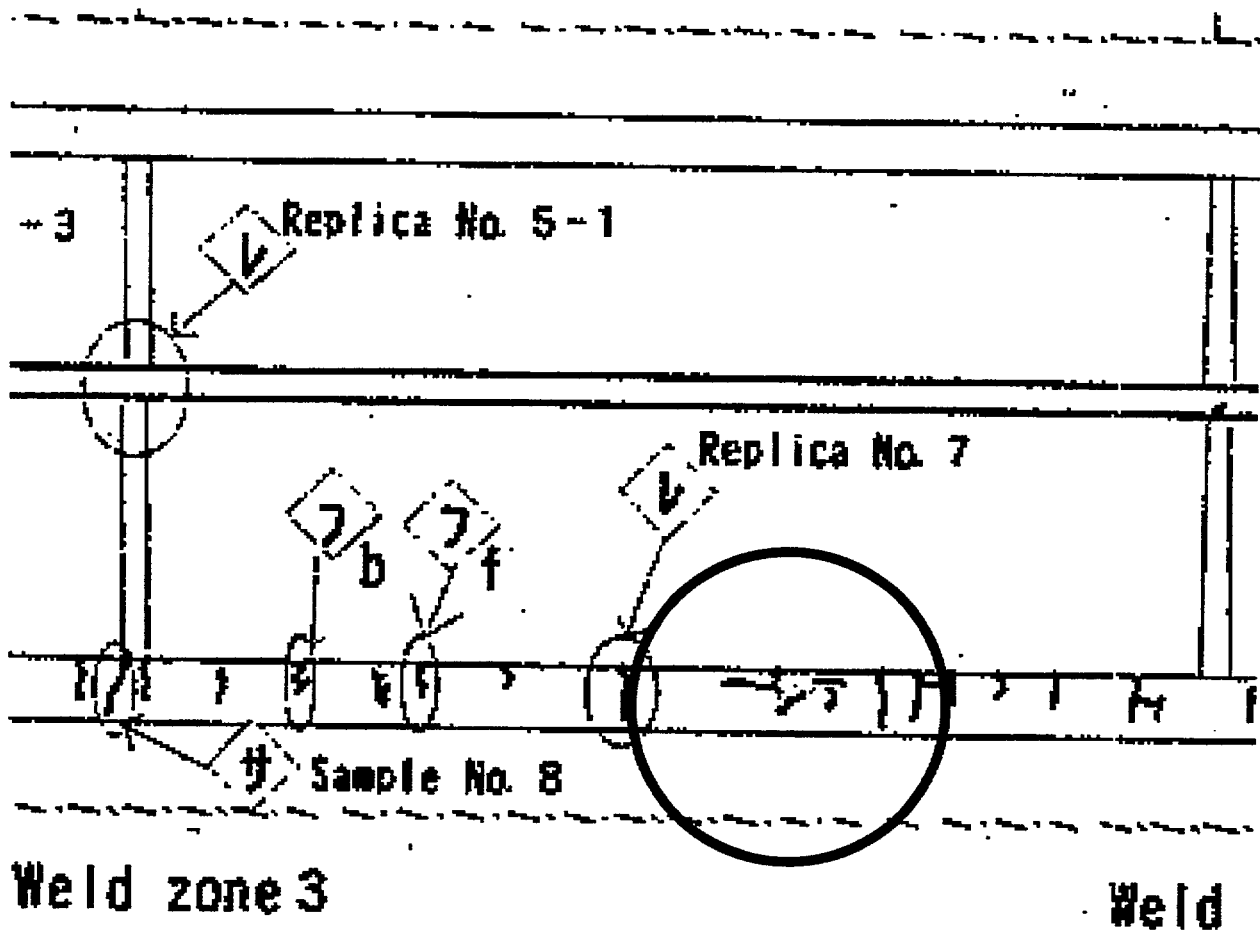


Figure 5-3: Schematic of the indications in the Tsuruga H9 weld region showing a series of circumferential indications that would overlap, having a UT length of 4-5 degrees

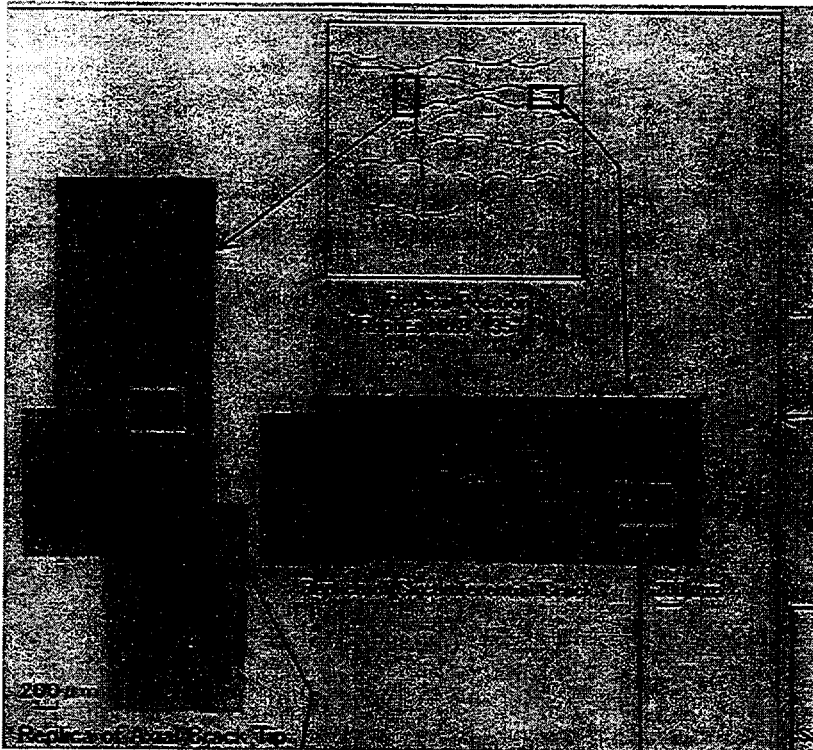


Figure 5-4: Replica metallography from circumferential crack and axial crack in the Tsuruga H9 weld region. The circumferential and axial cracking can be clearly linked due to the weld metal microstructure.

6. NMCA (NOBLECHEM™) EFFECTIVENESS FOR SHROUD SUPPORT CRACKING AT NMP-1

As stated earlier, Alloy 182 is used in both the H9 and H8 weld locations in NMP-1. It has been used extensively for the attachment welds used to join the shroud support structure to the RPV in most other BWRs as well. While it was initially selected due to its good corrosion resistance as well as its compatibility with both low alloy steel and austenitic stainless steel, it has been found over the last two decades to be highly susceptible to intergranular stress corrosion cracking (IGSCC) in high temperature oxygenated water environments. The purpose of this section is to confirm that the stress corrosion cracking is mitigated by hydrogen water chemistry (HWC) with NobleChem™, the environment currently present in NMP-1.

As discussed in BWRVIP-59 [Reference 5-1], the best accepted working hypothesis for the crack propagation process for IGSCC of Ni-base alloys follows that for types 304/316 austenitic stainless steel in high temperature water. This hypothesis presumes that these alloys crack via the film rupture/ slip oxidation mechanism, requiring the simultaneous presence of stress, susceptible material and oxidizing environment [Reference 5-1]. For Alloy 182 weldments, these three factors are known to have been present in the shroud support structure locations in NMP-1. In addition to susceptible material, the coolant environment was normal water chemistry (NWC) until 2000 and the weld would contain residual stresses from fabrication even though the H9 and H8 welds were subjected to post weld heat treatment (PWHT) which would be expected to reduce peak stresses.

The link that allows application of the stainless steel mechanism to Ni-base materials is based on the commonality in material characteristics and water chemistry effects. Intergranular (IGSCC) or interdendritic (IDSCC) cracking is the dominant failure mode in both materials. This has been shown to be associated with reduced chromium concentration at the boundaries as well as the amount of stabilizing element additions of niobium and titanium and the carbon level. These parameters have also been used to develop the more resistant alloys such as Alloy 82 that have exhibited high IGSCC resistance in the laboratory and the field, particularly relative to crack initiation. The understanding of these materials was discussed in BWRVIP-38, which made reference to earlier studies supporting these conclusions. The later report, BWRVIP-59, was much more comprehensive in its assessment of the nickel base alloys and added a significant amount of information as to the susceptibilities of the alloys and their crack growth rate characteristics.

In terms of crack growth rate studies, there have been many evaluations by several different laboratories including GE Nuclear Energy (GENE). BWRVIP-59 provided a

comprehensive summary of those tests in BWRVIP-59. The report also included assessments of field cracking, laboratory crack initiation tests, component tests, in-reactor crack growth tests and very importantly, efforts to model the SCC crack growth rates in these nickel base alloys. A significant thrust of the BWRVIP-59 effort was to characterize the benefits of effective hydrogen water chemistry (HWC) on crack growth rates. A brief discussion of these efforts and the conclusions follow, with the purpose of reiterating the technical positions that crack growth rates are significantly reduced in this mitigating HWC environment.

While the BWRVIP-38 report reviewed the cracking in field components, none of the data came from plants where HWC was present or present during the periods between inspections. The rates do, however, confirm the similarity of crack growth behavior between stainless steels and nickel base weld metals.

The larger effort was directed at using laboratory crack growth rate data to establish crack growth rates for use in disposition efforts. The review was divided into GENE efforts that were used with the NRC in early disposition efforts to the current data from different labs: ABB, Studsvik, VTT (Valtion Teknillinen Tutkimuskeskus, Technical Research Center of Finland), Toshiba and GE corporate research and development (CR&D). The latter data was previously compiled by EPRI with much of the testing and material conditions well documented by the investigator. The data covers a very large range of conductivity, corrosion potential, cyclic loading conditions and applied K level. Appropriate screens to exclude data for conditions that are outside the range expected in plant operation, were applied in the report. These screens included the removal of tests conducted in high conductivity, cyclic loading conditions, or with very high applied K levels as well as any data with large testing inconsistencies. This data was then used to develop crack growth rate curves for use in future disposition efforts. While the report developed curves for both normal water chemistry (NWC) as well as hydrogen water chemistry (HWC), those measured in HWC were found to be consistently lower than the 5×10^{-5} in/hr rate currently used in the disposition of cracking in NWC.

Figure 6-1 gives the curve applicable to HWC environment where water chemistry is maintained consistent with the EPRI Guidelines, including staying below the Action Level 1 requirements for conductivity and chloride and sulfate levels. Plotted along with this figure are GE Nuclear Energy data from lab tests as well as CAV (Crack Arrest Verification) data that clearly support the benefit of the HWC environment. Many of the tests by other investigators also support the benefit of the HWC environment. In some cases the benefit is masked in that the lab tests were performed in multiple environments and were complicated by very large correction ratios (greater than 5) used to account for the actual measured growth versus the rate measured indirectly with the test potential drop monitoring technique.

The highest confidence is given to recent data from the GE CRD lab that has been acquired in on-going efforts in measuring the crack growth rates for Alloy 182. Dr.

Andresen from CR&D has continued to perform these tests and report crack growth rate information. Specifically, his recent testing has been conducted in high purity environments that are typical of those found in operating plants. Figure 6-2 displays the rates of crack growth at both high corrosion potential and low corrosion potential. Crack growth was measured under NWC conditions with high purity water. More importantly, Dr. Andresen continues to confirm that the crack growth is mitigated at the low electrochemical corrosion potential (ECP) levels. Figure 6-3 provides further confidence and details of the crack advance at the low ECPs. The rates are very slow, less than 7×10^{-7} in/hr, well below the proposed BWRVIP-59 HWC crack growth rate.

The final building block supporting the reduced crack propagation rates is based on the results of deterministic modeling based on the GE PLEDGE model. This modeling was performed based on stainless steel behavior and the current knowledge of the mechanisms of SCC in nickel base weld metal. The calculations are shown in Figure 6-4. The lowest curve was generated with the PLEDGE model for an ECP of -230 mV, she. The model again supports the significant reduction of crack growth rates in HWC with NobleChemTM. This result is consistent with the data measured by Andresen. The figure also shows the factor of improvement that is attributed to the low corrosion potentials produced by HWC (particularly with NobleChemTM additions) when it is compared to the NWC predictions.

In summary all of this information taken together continues to support the benefit of HWC with NobleChemTM in mitigating IGSCC (IDSCC) in Ni-base Alloy 182 resulting in significant reduction in the crack growth rates. The presence of this environment in NMP-1 during operation reduces crack growth significantly in the weld metal, thereby reducing the likelihood that any crack will penetrate to the low alloy steel material.

Figure 6-1: K-dependent Disposition Curve for Alloy 182 in HWC at or below Action Level 1

Figure 6-2: The effect of corrosion potential on the crack growth rate of Alloy 182 weld metal in near-theoretical purity water. The shift to H₂-deaerated conditions produces an immediate and dramatic decrease in growth rate.

Figure 6-3. Crack length vs. time for Alloy 182 weld metal tested in 288 °C water containing 95 ppb H₂ showing the very well behaved nature of many of the crack growth observations at low corrosion potential / low crack growth rates. The measured rate is less than 5×10^{-9} mm/s (7×10^{-7} in/hr) at the low corrosion potential typical of HWC with NobelChem™.

Figure 6-4: Comparison of Crack Growth Rates in Alloy 182 made using the PLEDGE Model. The benefit of HWC (-230mV, she) is clearly shown by the lower line.

7. IMPACT OF ALLOY 182 CRACKING ON THE REACTOR PRESSURE VESSEL

7.1. BACKGROUND

During shroud replacement activities at Tsuruga-1, both visual inspections and liquid penetrant examinations were performed directly on the shroud support structure to evaluate its condition. When cracks were found, the inspection scope was increased. This allowed a thorough examination of the entire H9 region. The cracks which were confined to the inside lower bottom side of the weld, were generally axial in orientation with 10% of the flaws circumferential in orientation. (This is similar in many ways to NMP-1 if the low amplitude indications are actually axial in nature as discussed in Section 5). The access also allowed the examination to be expanded to fully research the five flaws with the longest length during the progressive grinding process used to remove each crack. It was found that none of crack depths were deeper than 44 mm and none of the cracks entered the vessel low alloy steel base metal adjacent to the weld metal. While it was accepted that the cracks could potentially enter the low alloy steel during future operation, this data confirmed that the scenarios that were assumed in BWRVIP-60 were bounding approaches. The investigation at Tsuruga also showed that the cracking was confined to Alloy 182 even though the plant had operated over 25 years. Finally, the findings confirmed that the observed cracking did not present any safety concerns. The earlier assessment showed that any postulated flaw, either axial or fully circumferential, could tolerate projected crack growth for many years and still be smaller than the ASME Code allowable flaw size. Overall the findings at NMP-1 were consistent with the Tsuruga-1 findings. The NMP-1 UT data indications are in the Alloy 182 weld. However, the NMP-1 UT inspection technique was not capable of inspecting low alloy steel. The findings also need to be considered in the context of the BWR experience where no cracking into the RPV has been found based on ASME Section XI required inservice inspections (ISI).

Therefore, a NMP-1 specific assessment using the approach generically presented in BWRVIP-60 [Reference 7-1] can be used to quantify the time for either an axial or circumferential flaw, placed at the depth of the clad-low alloy steel interface, to establish the time interval for continued operation.

Key steps in the crack growth evaluation are the determination of the appropriate stress distributions, calculation of the stress intensity factors as a function of crack depth based on the assumed stress distributions, and the crack growth calculation using appropriate relationships between stress intensity factor, K and the crack growth rate, da/dt . These steps are discussed next.

7.2. STRESS DISTRIBUTIONS

A crack is assumed with its deepest point at the clad to low alloy steel base metal interface. Therefore, the stress distributions of concern are those on the crack face as the crack is postulated to advance into the base metal. The stress sources at the H9 weld are the following: (1) internal pressure, (2) thermal expansion, (3) cladding, and (4) weld residual from the H9 weld.

Internal Pressure and Thermal Expansion

An axisymmetric finite element model of the NMP-1 vessel along with the conical shroud support was developed for this purpose. The nominal thickness of the base metal in the H9 weld region is 7.125 inches. Figure 7-1 shows the finite element model. The following values of normal condition internal pressure and temperature were used in the analysis: pressure 1030 psi, temperature 550°F. Figures 7-2 and 7-3 show the axial (with respect to RPV axis) and circumferential (hoop) stress distributions for the preceding internal pressure and temperature loadings. The membrane and bending stress distributions are shown in Table 7-1.

Cladding Stress

BWRVIP-60 suggests that tensile stresses at 550°F can range from a low of 5 ksi (corresponding to a room temperature residual stress of 30 ksi) to approximately 20 ksi (corresponding to a room temperature residual stress of 45 ksi). Therefore, a conservative value of 20 ksi was used in this evaluation. A compressive stress of approximately 1 ksi was assumed in the base metal, balancing the 20 ksi tensile stress in the clad. This stress distribution is schematically shown in Figure 7-4. The thickness of the clad was assumed as 3/8 inch that is equal to the thickness of the pad.

Weld Residual Stress

The weld residual stress of importance in this evaluation is that in the base metal. The results of an experimental and analytical determination of H9 weld residual stresses for a vessel with a horizontal type of shroud support are reported in BWRVIP-60. These results show a high stress in the pad region followed by less than 8 ksi tensile or compressive stress in most of the base metal. Most likely the high stress in the pad region is associated with the thermal expansion coefficient difference between the Alloy 182 pad and the low alloy steel base metal which was already accounted for in the clad stress. BWRVIP-60 used a cosine function weld residual stress distribution with a peak value of 8 ksi. The same distribution is used in this evaluation and is shown in Figure 7-5. This stress distribution was characterized in a polynomial form as a function of distance 'x' measured from the clad-base metal interface:

$$\sigma_{\text{weld residual}} = (10.148) - 8.815 (x) + 1.2372 (x)^2$$

7.3. K CALCULATIONS

The stress intensity factor calculation procedures are described in this section. The calculations were conducted for an axial flaw with an aspect ratio of 0.1. This flaw geometry was determined to be the limiting one from the allowable flaw and the crack growth perspective.

Calculation of K due to Clad Stress

The stress intensity factor for the clad stress was first calculated using a point force on an edge-cracked plate (see Figure 7-6) and then corrected for cylindrical geometry. The K for the edge-cracked model were calculated using the following expression from Tada and Paris Handbook (Reference 7-2):

$$\begin{aligned} K &= \{2P/\sqrt{(\pi a)}\} F(a/b), \text{ where} & (2) \\ F(a/b) &= \{0.46 + 3.06 (a/b) + 0.84 (1-a/b)^5 + 0.66 (a/b)^2 (1-a/b)^2\} / \\ &\quad \{1 - a/b\}^{1.5} \end{aligned}$$

The 'a' and 'b' are as indicated in Figure 7-6. The K values predicted by the preceding equations are conservative for a crack in a cylindrical geometry. The conservatism was quantified by taking the ratio of the F₁ functions (for constant stress) for a flat plate versus a cylinder from Reference 7-3.

$$K = F_1 A_0 \sqrt{(\pi a)} \quad (3)$$

$$F_{1,\text{flat plate}}/F_{1,\text{cylinder}} = 1.0 + 0.5533 (x) - 2.7641 (x)^2 + 4.862 (x)^3 \quad (4)$$

Where, $x=a/b$. The calculated values of K from the edge-cracked plate model (Equation 2) were reduced by the ratio predicted by Equation (4).

The K due to compressive stress was calculated using the approach of Reference 7-5. The overall K was then calculated for any crack length and is shown in Figure 7-7. Note that the value of 'a' in Figure 7-7 is based on distance from the clad-base metal interface. Figure 7-7 also shows the polynomial fit to the K values.

Calculation of K due to Weld Residual and Normal Operation Stresses

The K values for the weld residual stresses and the internal pressure plus thermal case were calculated using the Raju and Newman method for an axial flaw in a cylinder (Reference 7-4):

$$K_1 = [\sqrt{\{(\pi a)/Q\}}] (G_0 A_0 a^0 + G_1 A_1 a^1 + G_2 A_2 a^2 + G_3 A_3 a^3) \quad (5)$$

The hoop stress, σ_θ is characterized in a polynomial form as follows:

$$\sigma_\theta = A_0x^0 + A_1x^1 + A_2x^2 + A_3x^3 \quad (6)$$

where, 'x' is the distance from the clad-base metal interface. G_0, G_1, G_2 and G_3 are non-dimensional coefficients which are a function of crack aspect ratio for a given radius to thickness (R/t) ratio. The Raju-Newman solution gives these coefficients for a R/t ratio of 10. The NMP-1 R/t ratio in H9 weld region is approximately 15. However a check of the coefficients given in Reference 7-5 for a uniform stress with R/t of 10 and R/t of 15 showed insignificant difference for the range of crack depths considered in this evaluation. The G functions in the Raju and Newman paper are given as discrete values. The following polynomial fits were used for the case with aspect ratio of 0.1:

$$\begin{aligned} G_0 &= 0.9809 + 0.5228 (a/t) + 0.7389 (a/t)^2 \\ G_1 &= 0.6369 + 0.1061 (a/t) + 0.3722 (a/t)^2 \\ G_2 &= 0.4999 + 0.0228 (a/t) + 0.2389 (a/t)^2 \end{aligned}$$

The value of 'Q' in Equation (5) was calculated as prescribed in Appendix A of ASME Section XI [Reference 7-6]. The calculated values of K from weld residual and normal operation were then combined with the K values from clad stress to obtain the total value of K.

Total Value of K

As stated earlier, the total value of applied stress intensity factor K was obtained by summing the contributions from the weld residual and normal operation stresses, and the clad stresses. The values of total K as a function of crack depth 'a' are shown in Figure 7-8. Also shown in this Figure is the polynomial fit to the K values.

7.4. CRACK GROWTH CALCULATIONS

The K values as a function of 'a' represented in Figure 7-8 were used in the crack growth rate calculations. The following K versus da/dt relationships from BWRVIP-60 were used to calculate the crack growth rate:

$$\begin{aligned} da/dt &= 2.8 \times 10^{-6} && \text{in/hour for } K < 50 \text{ ksi}\sqrt{\text{in}} \\ &= 6.82 \times 10^{-12} (K)^4 && \text{in/hour for transient conditions or } K \geq 50 \text{ ksi}\sqrt{\text{in}} \end{aligned}$$

For the purpose of the crack growth calculation it was assumed that there will be approximately 800 hours of transient condition operation during a 2-year (16000 hours) cycle of operation. The results of crack growth prediction are shown in Figure 7-9. The initial crack depth is equal to the thickness of the pad that is 0.375 inch. The operating

time before the postulated indication at the clad-base metal interface is predicted to grow to the allowable crack depth is discussed next.

7.5. IWB-3600 EVALUATION

The allowable flaw per IWB-3600 of the ASME code [Reference 7-6] procedures can be calculated by determining the crack length at which the applied K reaches a value equal to the K_{IR} value with appropriate safety factor. It was determined that the normal/upset condition provides the limiting condition for which the required safety factor is $\sqrt{10}$ or 3.16. At the normal/upset conditions the RPV material in the H9 weld region is expected to be in the upper shelf region with a bounding value of K_{IR} as 200 ksi $\sqrt{\text{in}}$. Therefore, the allowable K value is $200/\sqrt{10}$ or 63.2 ksi $\sqrt{\text{in}}$. A review of Figure 7-8 indicates that this gives an allowable crack depth of approximately 2 inches. Figure 7-9 indicates that this value of crack depth is reached in excess of 200,000 hours of operation. This clearly demonstrates that there is a significant margin in terms of operating hours before a hypothetical indication at the clad-base metal interface could reach allowable depth in the base metal determined by IWB-3600 procedures.

7.6. REFERENCES

- [7-1] "BWR Vessel and Internals Project, Evaluation of Stress Corrosion Crack Growth in Low Alloy Steel Vessel Materials in the BWR Environment (BWRVIP-60," EPRI TR-108709, March 1999.
- [7-2] Tada, H., Paris, P. and Irwin, G., "The Stress Analysis of Cracks Handbook," Del Research Corporation (1985).
- [7-3] Buchalet, C.B. and Bamford, W.H., "ASTM 8th National Symposium on Fracture Mechanics, 1974", ASTM STP-590 (1975).
- [7-4] Raju, I.S. and Newman, J.C., "Stress intensity Factor Influence coefficients for Internal and External Surface Cracks in Cylindrical Vessels," ASME PVP-58 (1982).
- [7-5] "An Engineering Approach for Elastic-Plastic Fracture Analysis," EPRI NP-1931, July 1981.
- [7-6] ASME Boiler and Pressure Vessel Code, Section XI, Rules for In-Service Inspection of Nuclear Power Plant Components, American Society of Mechanical Engineers.

Table 7-1 Stresses Due to Internal Pressure and Temperature in the RPV at H9 Weld

	Axial Stress (psi)	Circumferential Stress (psi)
Inside	-12170	13900
Outside	26810	26840
Membrane	7320	20370
Bending	-19490	-6470

Table 7-2 Coefficients for K calculation

Stress	A ₀	A ₁	A ₂
Weld Residual	10.148	-8.815	1.237
Normal Op.	13.400	1.853	-
Total	23.548	-6.962	1.237

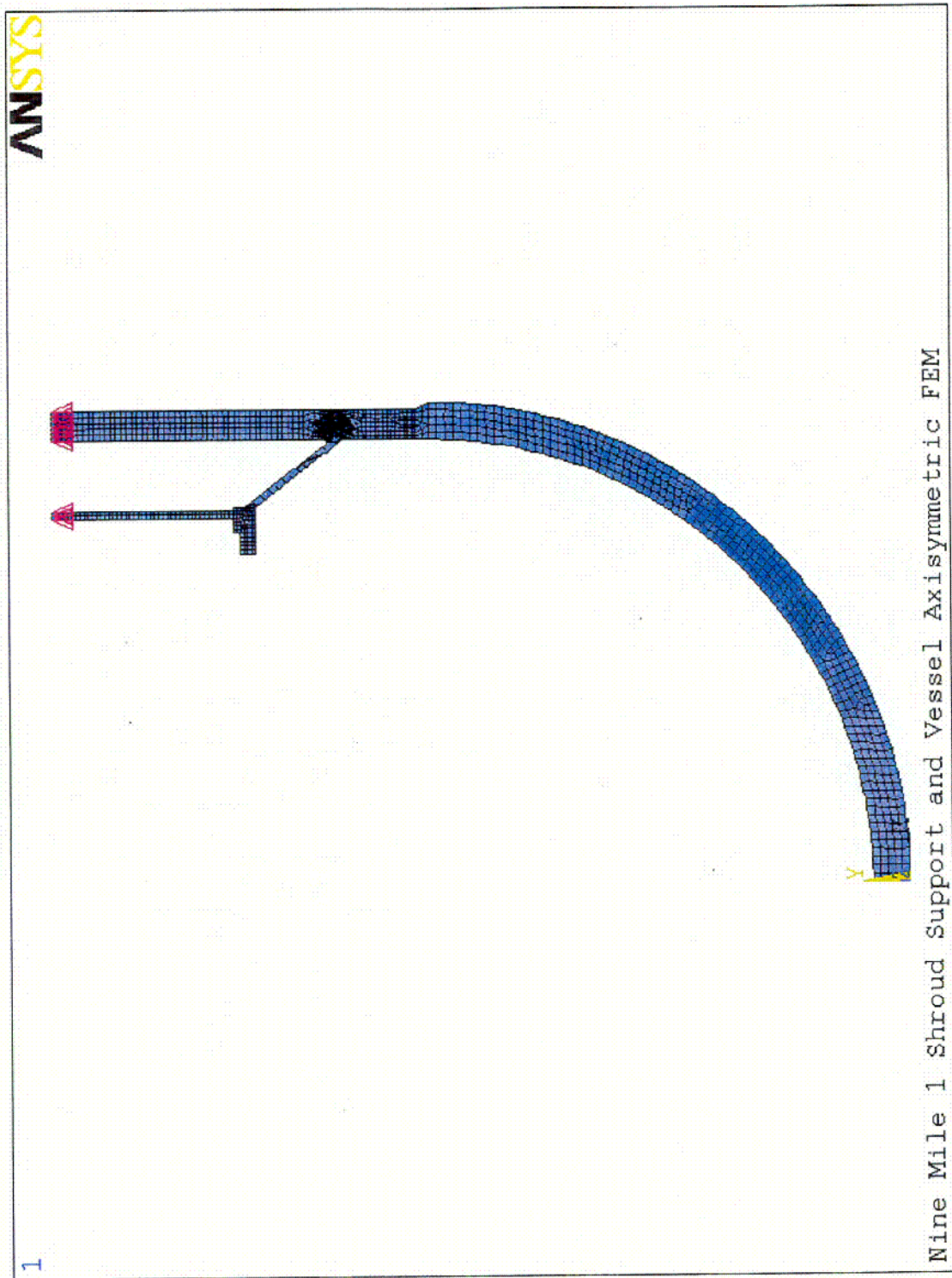


Figure 7-1 Axisymmetric Finite Element Model of RPV Including The Conical Shroud Support

ANSYS 5.6
 APR 12 2001
 13:56:23
 ELEMENT SOLUTION
 STEP=1
 SUB =1
 TIME=1
 SY (NOAVG)
 RSYS=0
 PowerGraphics
 EFACET=1
 DMX = .627376
 SMN = -52791
 SMX = 24754
 -52791
 -44175
 -35559
 -26942
 -18326
 -9710
 -1094
 7522
 16138
 24754

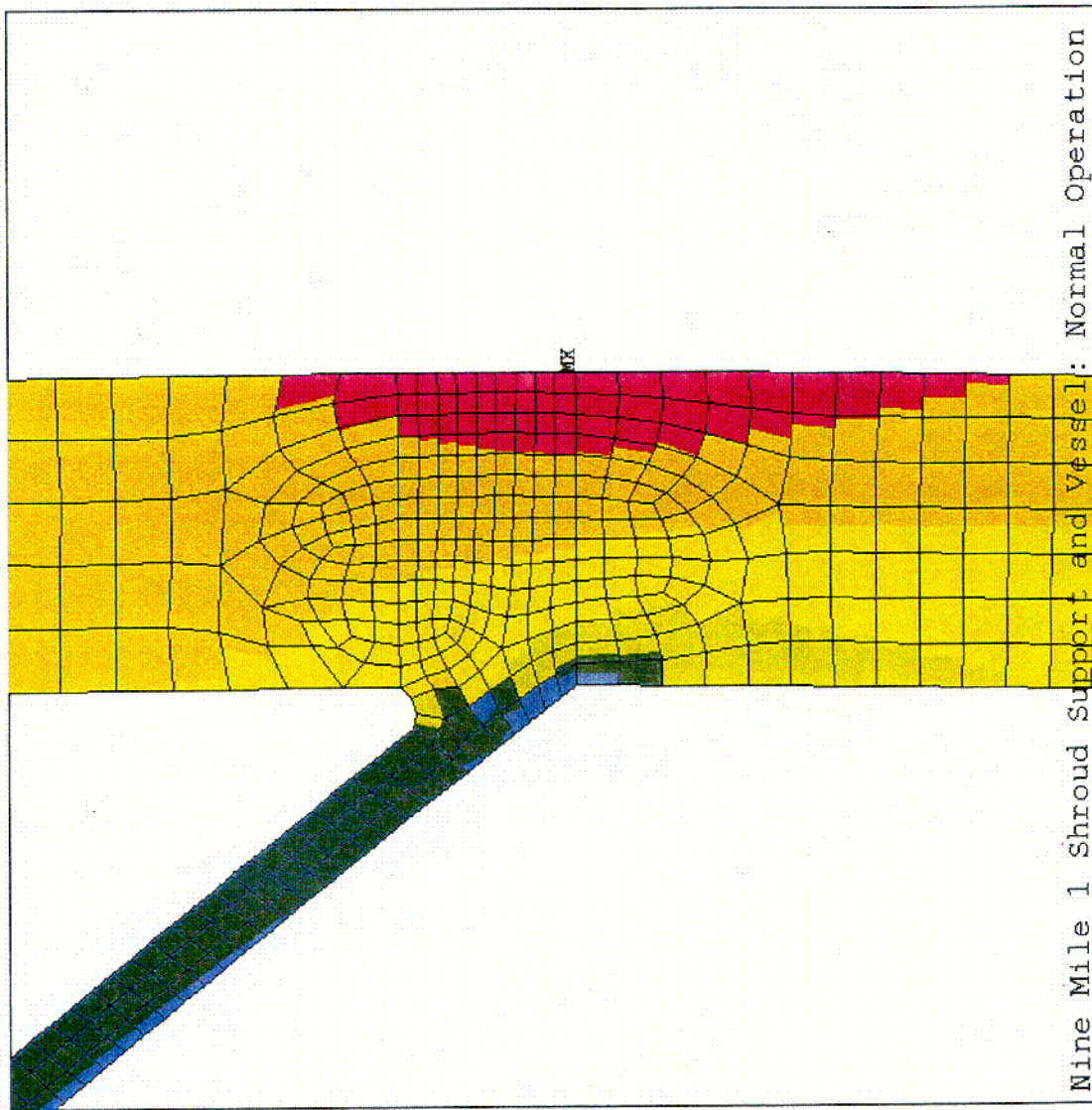


Figure 7-2 Axial (Y) Stress Distribution Due to Pressure and Temperature at Normal Operation

ANSYS 5.6
APR 12 2001
13:58:13
ELEMENT SOLUTION
STEP=1
SUB =1
TIME=1
SZ (NOAVG)
RSYS=0
PowerGraphics
EFACET=1
DMX =.627376
SMN =-46554
SMX =25782
-46554
-38517
-30480
-22442
-14405
-6368
1670
9707
17744
25782

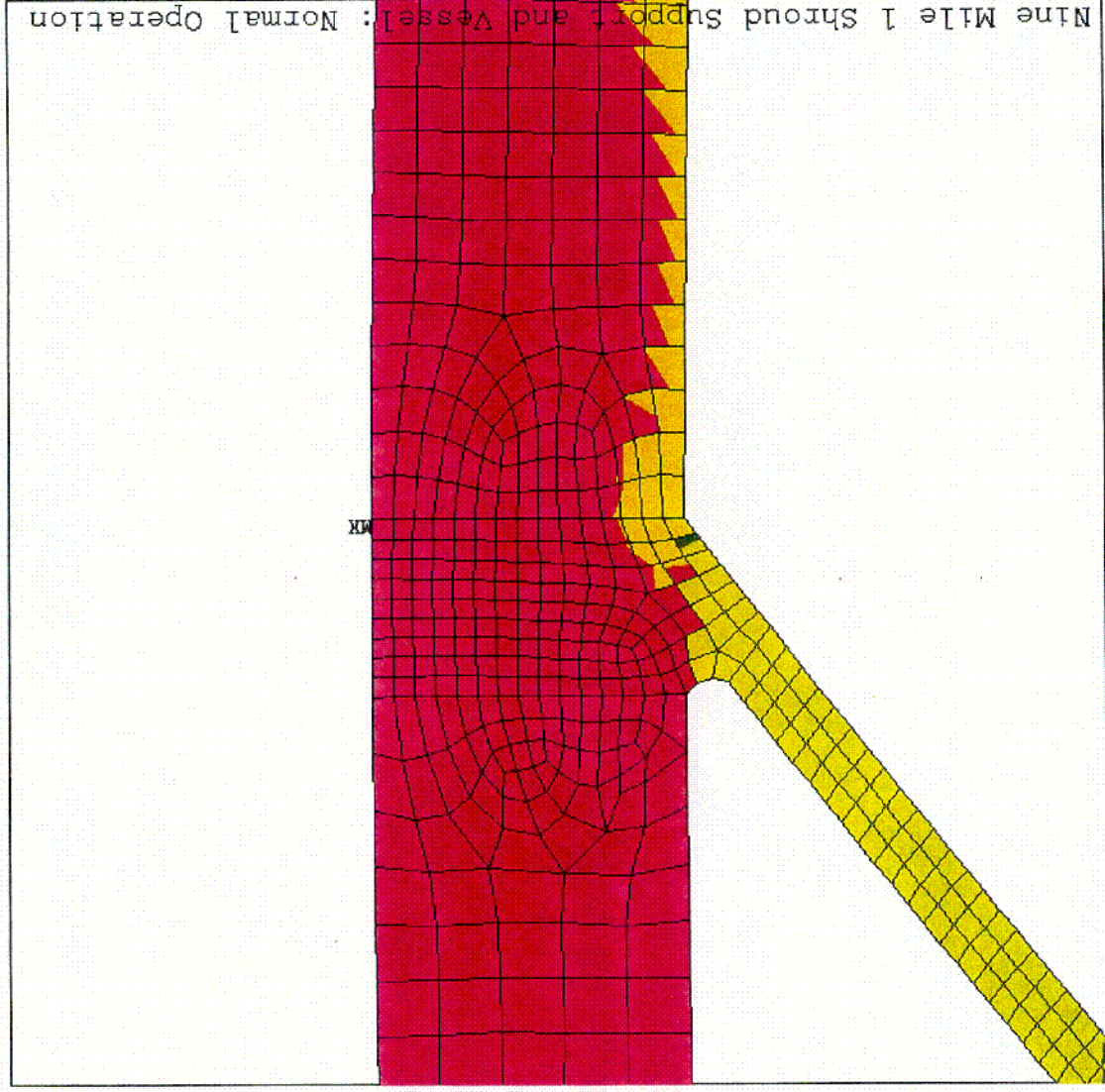


Figure 7-3 Circumferential (Z) Stress Distribution Due to Pressure and Temperature at Normal Operation

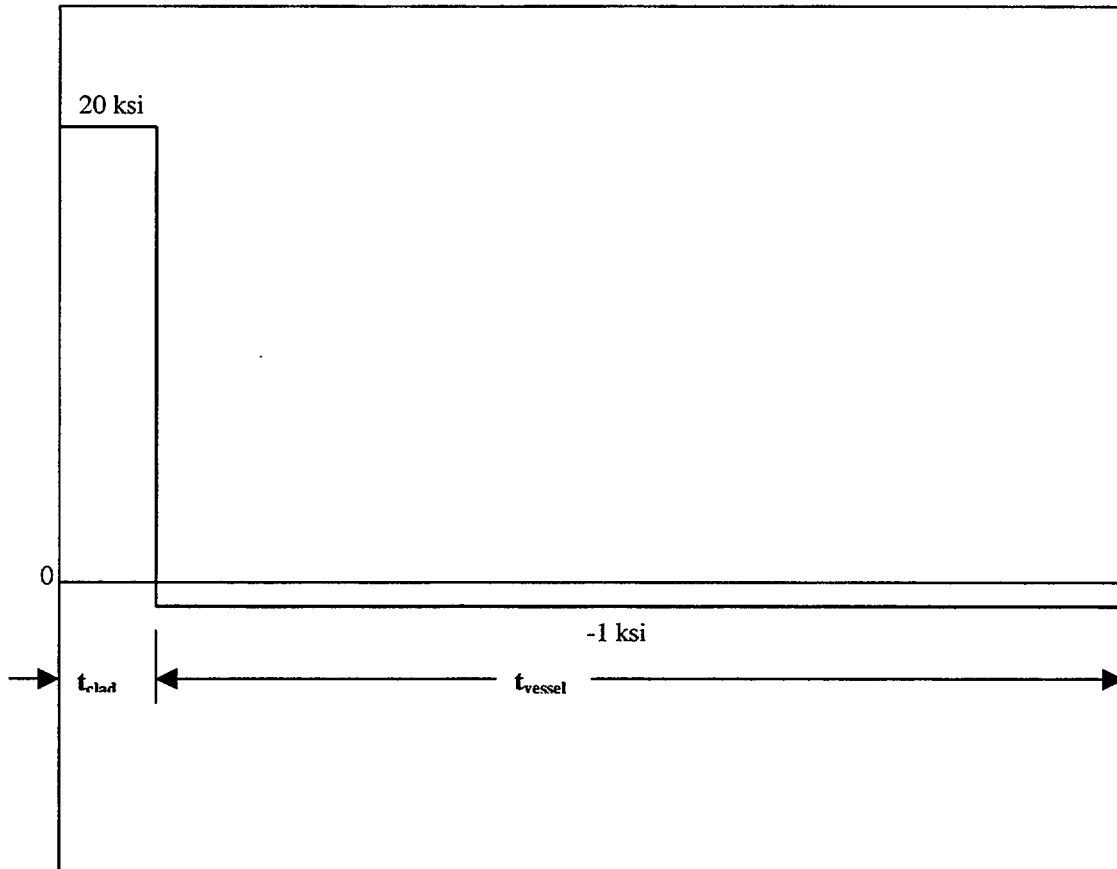


Figure 7-4: Assumed Clad Residual Stress Distribution

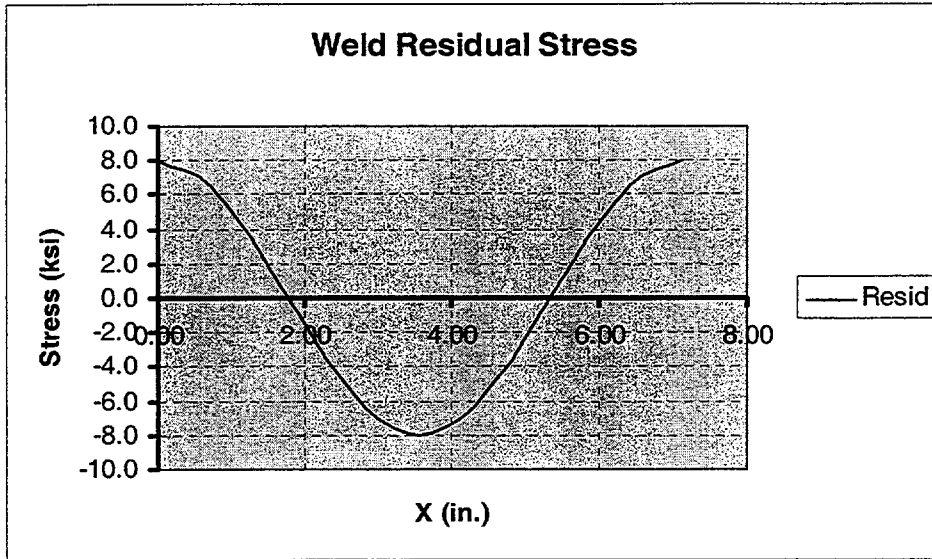
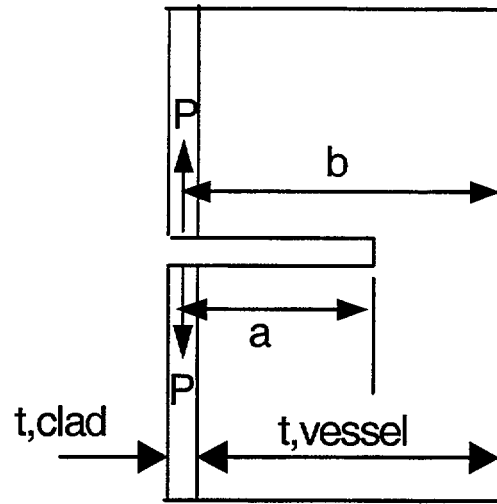


Figure 7-5 Assumed Weld Residual Stress Distribution



$$P = (\text{Clad Stress}) \times (t, \text{clad})$$

Figure 7-6 Edge Cracked Plate Model for K Calculation Due to Clad Stress

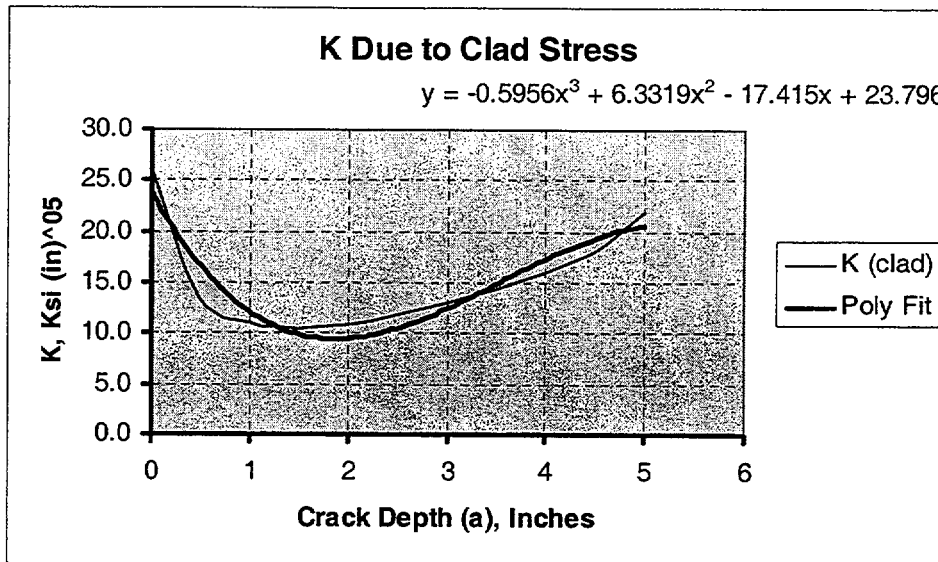


Figure 7-7 K Due to Clad Stress and Polynomial Fit

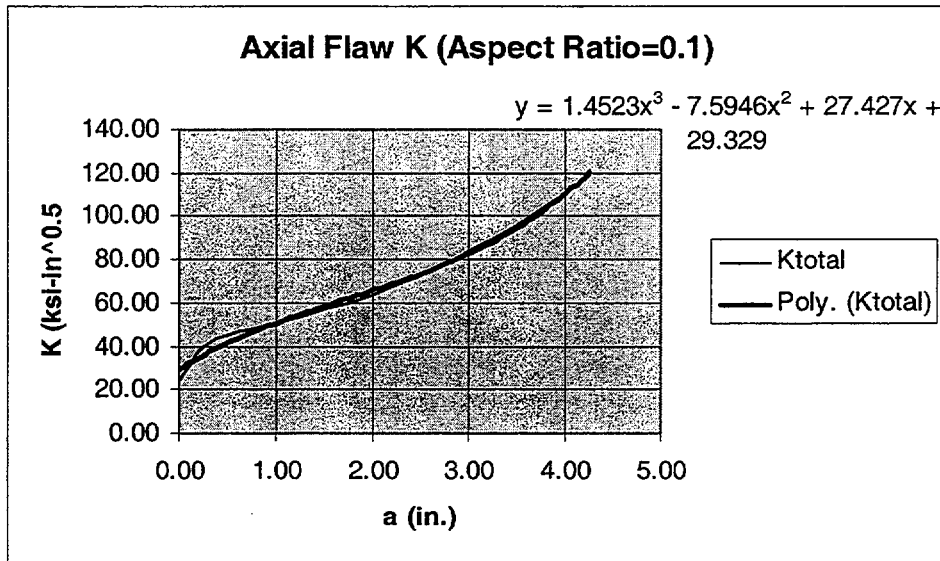


Figure 7-8 Calculated Values of Total K and the Polynomial Fit

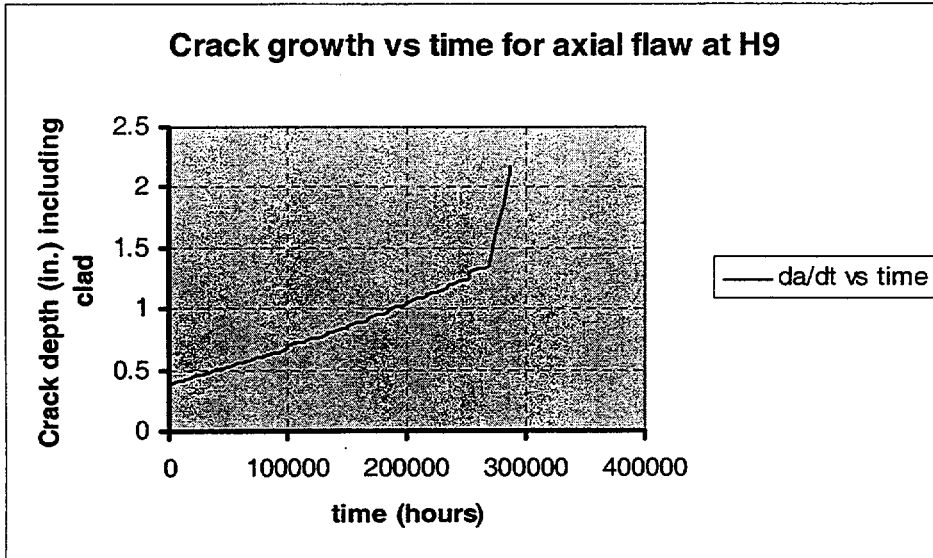


Figure 7-9: Crack Growth Prediction as a Function of Operating Hours

8. REINSPECTION RECOMMENDATIONS

The H9 weld inspections fall under ASME Section XI, category B-N-2 in Table IWB-2500-1, which requires single sided VT-3 visual inspection. The NMP-1 H9 weld inspections were performed to the more stringent BWRVIP-38 H9 weld inspection requirements. BWRVIP-38 recommends supplemental inspection using volumetric techniques if cracking is identified in the H9 weld to confirm no penetration to the low alloy steel. BWRVIP-38 also recognizes analysis if inspection cannot be performed. In addition, paragraph IWB-2420 of Section XI provides guidance when the component acceptance for continued service is based on an analytical evaluation such as presented in Section 7 of this report. This analytical evaluation shows significant structural margins for a plant operating period in excess of 100,000 hours even if cracking to the vessel material is assumed and conservatively assuming the potential for crack growth into low alloy steel.

Volumetric re-inspection from the OD of the vessel at the H9 weld can only be performed in the vicinity of the recirculation suction nozzles. At these locations, OD inspection can provide access to the H9 weld for volumetric inspection to establish the condition of the low alloy steel (LAS) material at the H9 weld. The analysis performed establishes a high degree of flaw tolerance for H9 vessel attachment weld cracking, extremely low probability of LAS penetration and slow potential crack growth potential into the LAS. Based on this evaluation, continued operation for at least one operating cycle prior to volumetric inspection from the vessel OD on a sampling basis is justified.

9. CONCLUSIONS

There were several objectives and outcomes of this effort as given below:

- (1) First, the structural margin at the H9 weld was evaluated using the DLL computer program and methodology consistent with BWRVIP-38. A conservative crack growth rate of 5×10^{-5} in/hour was used. This crack growth rate was also conservatively applied at each end of the uninspected areas that were assumed to be through-wall cracked. The structural margin, after factoring in the crack growth for 10 years of operation, was considerably in excess of the required margin.
- (2) The second effort established that the presence of axial cracking at weld H9 has insignificant effect on the flaw tolerance for circumferential cracking.
- (3) A fracture mechanics evaluation was conducted for potential crack growth into the reactor vessel wall. The evaluation methodology was consistent with BWRVIP-60 and the allowable crack depth was based on IWB-3600 of ASME Section XI. The evaluation showed

that crack depth in the reactor wall is predicted to be less than the allowable value even after an operating period in excess of 100,000 hours.

(4) An evaluation of the orientation of cracking, based on the UT results from NMP-1, and the dye penetrant and metallurgical results from Tsuruga-1, show that the mechanism of cracking is expected to be the same. The extent of circumferential cracking is also similar, taking into account the overlapping indications found at Tsuruga and the predominance of indications with low UT amplitude in the NMP-1 examination.

(5) A review of the understanding of the effectiveness of HWC, with NobleChem™, confirms that as a result of the application of HWC future rates of SCC in Alloy 182 weld metal will be significantly reduced over previous rates. This adds margin to the evaluation performed.

ATTACHMENT D

AFFIDAVIT

General Electric Company

AFFIDAVIT

I, **David J. Robare**, being duly sworn, depose and state as follows:

- (1) I am Technical Projects Manager, General Electric Company ("GE") and have been delegated the function of reviewing the information described in paragraph (2) which is sought to be withheld, and have been authorized to apply for its withholding.
- (2) The information sought to be withheld is contained in the GE proprietary report GE-NE-B13-02097-00, Section 5, *The Evaluation of Observed Cracking at Nine Mile Point Unit 1 H9 Weld for Continued Operation*, Revision 1, Class III (GE Nuclear Energy Proprietary Information), dated July 2001. The proprietary information is delineated by bars marked in the margin adjacent to the specific material.
- (3) In making this application for withholding of proprietary information of which it is the owner, GE relies upon the exemption from disclosure set forth in the Freedom of Information Act ("FOIA"), 5 USC Sec. 552(b)(4), and the Trade Secrets Act, 18 USC Sec. 1905, and NRC regulations 10 CFR 9.17(a)(4), 2.790(a)(4), and 2.790(d)(1) for "trade secrets and commercial or financial information obtained from a person and privileged or confidential" (Exemption 4). The material for which exemption from disclosure is here sought is all "confidential commercial information", and some portions also qualify under the narrower definition of "trade secret", within the meanings assigned to those terms for purposes of FOIA Exemption 4 in, respectively, Critical Mass Energy Project v. Nuclear Regulatory Commission, 975F2d871 (DC Cir. 1992), and Public Citizen Health Research Group v. FDA, 704F2d1280 (DC Cir. 1983).
- (4) Some examples of categories of information which fit into the definition of proprietary information are:
 - a. Information that discloses a process, method, or apparatus, including supporting data and analyses, where prevention of its use by General Electric's competitors without license from General Electric constitutes a competitive economic advantage over other companies;
 - b. Information which, if used by a competitor, would reduce his expenditure of resources or improve his competitive position in the design, manufacture, shipment, installation, assurance of quality, or licensing of a similar product;

- c. Information which reveals cost or price information, production capacities, budget levels, or commercial strategies of General Electric, its customers, or its suppliers;
- d. Information which reveals aspects of past, present, or future General Electric customer-funded development plans and programs, of potential commercial value to General Electric;
- e. Information which discloses patentable subject matter for which it may be desirable to obtain patent protection.

The information sought to be withheld is considered to be proprietary for the reasons set forth in both paragraphs (4)a. and (4)b., above.

- (5) The information sought to be withheld is being submitted to NRC in confidence. The information is of a sort customarily held in confidence by GE, and is in fact so held. The information sought to be withheld has, to the best of my knowledge and belief, consistently been held in confidence by GE, no public disclosure has been made, and it is not available in public sources. All disclosures to third parties including any required transmittals to NRC, have been made, or must be made, pursuant to regulatory provisions or proprietary agreements which provide for maintenance of the information in confidence. Its initial designation as proprietary information, and the subsequent steps taken to prevent its unauthorized disclosure, are as set forth in paragraphs (6) and (7) following.
- (6) Initial approval of proprietary treatment of a document is made by the manager of the originating component, the person most likely to be acquainted with the value and sensitivity of the information in relation to industry knowledge. Access to such documents within GE is limited on a "need to know" basis.
- (7) The procedure for approval of external release of such a document typically requires review by the staff manager, project manager, principal scientist or other equivalent authority, by the manager of the cognizant marketing function (or his delegate), and by the Legal Operation, for technical content, competitive effect, and determination of the accuracy of the proprietary designation. Disclosures outside GE are limited to regulatory bodies, customers, and potential customers, and their agents, suppliers, and licensees, and others with a legitimate need for the information, and then only in accordance with appropriate regulatory provisions or proprietary agreements.
- (8) The information identified in paragraph (2), above, is classified as proprietary because it contains detailed results of analytical models, methods and processes, including computer codes, which GE has developed and applied to perform flaw evaluations for the BWR.

The development of flaw evaluation methodology that are used to evaluate BWRs was achieved at a significant cost to GE.

The development of the evaluation process contained in the paragraph (2) document along with the interpretation and application of the analytical results is derived from the extensive experience database that constitutes a major GE asset.

- (9) Public disclosure of the information sought to be withheld is likely to cause substantial harm to GE's competitive position and foreclose or reduce the availability of profit-making opportunities. The information is part of GE's comprehensive BWR safety and technology base, and its commercial value extends beyond the original development cost. The value of the technology base goes beyond the extensive physical database and analytical methodology and includes development of the expertise to determine and apply the appropriate evaluation process. In addition, the technology base includes the value derived from providing analyses done with NRC-approved methods.

The research, development, engineering, analytical and NRC review costs comprise a substantial investment of time and money by GE.

The precise value of the expertise to devise an evaluation process and apply the correct analytical methodology is difficult to quantify, but it clearly is substantial.

GE's competitive advantage will be lost if its competitors are able to use the results of the GE experience to normalize or verify their own process or if they are able to claim an equivalent understanding by demonstrating that they can arrive at the same or similar conclusions.

The value of this information to GE would be lost if the information were disclosed to the public. Making such information available to competitors without their having been required to undertake a similar expenditure of resources would unfairly provide competitors with a windfall, and deprive GE of the opportunity to exercise its competitive advantage to seek an adequate return on its large investment in developing these very valuable analytical tools.

STATE OF CALIFORNIA)
)
COUNTY OF SANTA CLARA) ss:

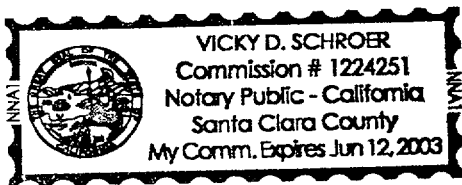
David J. Robare, being duly sworn, deposes and says:

That he has read the foregoing affidavit and the matters stated therein are true and correct to the best of his knowledge, information, and belief.

Executed at San Jose, California, this 19TH day of JULY 2001.

David J. Robare
David J. Robare
General Electric Company

Subscribed and sworn before me this 19th day of July 2001.



Vicky D. Schroer
Notary Public, State of California